

1 **ABSTRACT**

2 In this work, the degradation of cefalexin, norfloxacin, and ofloxacin was examined via various advanced
3 oxidation processes (AOPs). Direct photolysis by ultraviolet (UV) and vacuum ultra violet (VUV) was less
4 effective for the degradation of fluoroquinolone antibiotics such as norfloxacin and ofloxacin than that of
5 cefalexin. Both hydrogen peroxide (H_2O_2) and potassium persulfate ($\text{K}_2\text{S}_2\text{O}_8$) assisted UV/VUV process
6 remarkably enhanced fluoroquinolone degradation. The addition of $\text{K}_2\text{S}_2\text{O}_8$ was superior to H_2O_2 under VUV
7 irradiation, with the best removal efficiency of norfloxacin and ofloxacin being almost 100% within 3 min in
8 the presence of VUV/ $\text{K}_2\text{S}_2\text{O}_8$. The ofloxacin degradation rate was accelerated as concentrations of H_2O_2 and
9 $\text{K}_2\text{S}_2\text{O}_8$ was increased to 3 mM, but the degradation rate was slightly decreased with excess H_2O_2 (> 3 mM).
10 The performance of modified VUV processes (*i.e.*, VUV/ H_2O_2 and VUV/ $\text{K}_2\text{S}_2\text{O}_8$) was inhibited at highly
11 alkaline condition (pH 11). The co-existence of halides (Cl^- and Br^-) enhanced antibiotics degradation via the
12 modified VUV processes, but the reaction was almost unaffected in the presence of single halides. This study
13 demonstrated that modified VUV processes (especially VUV/ $\text{K}_2\text{S}_2\text{O}_8$) are efficient for eliminating
14 fluoroquinolone antibiotics from water, which can be considered as a clean and green method for the treatment
15 of antibiotics-containing industrial wastewater.

16 **Keywords:** fluoroquinolone antibiotics; persulfate radicals; chlorides/bromides; vacuum-ultraviolet light;
17 catalytic degradation; sustainable remediation.

18 **1. Introduction**

19 Discharge of pollutants from a variety of industries to soil, water, and air has increased the importance of
20 using proper treatment for pollutants with different characteristics (Hou et al., 2017; Song et al., 2018; Zhang
21 et al., 2018). In particular, pharmaceutical and personal care products (PPCPs) have been an emerging concern
22 due to their harmful effects on aquatic organisms and human health (Jin et al., 2018). Water contamination
23 associated with PPCPs has become a serious problem due to increasing population and rapid industrialization
24 in many countries. Among the broad span of PPCPs, antibiotics that easily enter into water matrices have
25 gained considerable attention because of their extensive use in field and persistent nature (Sun et al., 2017;
26 Copete-Pertuz et al., 2018; Guo et al., 2018). Long-term exposure to antibiotics in the environment may
27 increase the number of antibiotic-resistant bacteria (Zhu et al., 2015). The occurrence and risk assessment of
28 sixteen antibiotics had been surveyed in several sewage treatment plants (STPs) in Hong Kong, where the
29 major antibiotics were found to be cefalexin (CEX) and ofloxacin (OFX) (Leung et al., 2012). Norfloxacin
30 (NOF) is a fluoroquinolone antibacterial agent ubiquitously detected in drinking water/wastewater and its
31 bioaccumulation could pose a serious threat to the public health, aquatic organisms, and wildlife (Ahmed et
32 al., 2014; Sun et al., 2017). Thus, one of the recent focuses of research is laid on the removal of antibiotics
33 from water.

34 Non-biotic treatment methods that are able to eliminate antibiotics have been mainly considered since
35 antibiotics are mostly designed to have strong resistance to hydrolysis, which is important for transformation
36 of common organic pollutants in water (Ghauch et al., 2017). A variety of techniques including adsorption
37 (Yan and Niu, 2018), electrochemical degradation (Lan et al., 2017), and oxidation processes (Lofrano et al.,
38 2018) have been used to remove antibiotics from water. Among these techniques, oxidation processes
39 including ultraviolet (UV) irradiation, hydrogen peroxide (H₂O₂), Fenton reaction (Fe(II)/H₂O₂), and ozone
40 (O₃) have drawn great interest due to their high removal efficiencies for antibiotics (Mondal et al., 2018).

41 Advanced oxidation processes (AOPs) can degrade a variety of organic contaminants into less complex
42 byproducts and finally mineralize them into carbon dioxide and water in both surface water and wastewater
43 (Dhaka et al., 2018). Various UV-based processes can be significantly enhanced by the combination of
44 technologies (MacDonald et al., 2018). UV process can overcome several problems in the other processes,
45 such as long reaction time in biological processes, sludge production in coagulation process, regeneration of
46 adsorbent in adsorption process, and acidic condition in Fenton oxidation (Rodríguez-Chueca et al., 2018).
47 UV irradiation has been frequently used for drinking water purification due to its excellent removal
48 efficiencies for aquatic pathogens and organic pollutants, which has the potential to be an economically
49 feasible wastewater treatment process (Yuval et al., 2017).

50 To improve the degradation efficiency, the use of vacuum UV (VUV) irradiation at the wavelength of 185
51 nm as a promising alternative to UV irradiation (254 nm) has been investigated recently because it generates
52 a large amount of reactive species via activation of water molecules (Xie et al., 2018). The VUV process
53 generates both hydroxyl radical ($\cdot\text{OH}$) and aqueous electrons (e^-) via homolysis/ionization of water molecules
54 (viz. $\text{H}_2\text{O} + \text{VUV}_{185} \rightarrow \cdot\text{OH} + \text{H}\cdot$; $\text{H}_2\text{O} + \text{VUV}_{185} \rightarrow \cdot\text{OH} + \text{H}^+ + e^-$; $\text{H}\cdot + \text{H}_2\text{O} \rightarrow \text{H}_3\text{O}^+ + e^-$) (Kosma et al.,
55 2015), and the oxidation rate of pollutants can be accelerated by these reactive species. The effectiveness of
56 homogeneous VUV-based AOP in the degradation of antibiotics has been validated. For example, Pourakbar
57 et al. (2016) observed efficient degradation and mineralization of amoxicillin by VUV irradiation under
58 different solution pHs, initial amoxicillin concentrations, water ingredients, and hydraulic retention times
59 (HRTs). The performance of VUV photolysis in the removal of acetaminophen in the presence of nitrate was
60 evaluated using a continuous-flow photoreactor in which acetaminophen was completely oxidized with
61 nitrate reduction to N_2 (~99%) at 80 min-HRT (Moussavi et al., 2016).

62 External chemical addition in UV-based process have also been tried to enhance the degradation efficiency.
63 In particular, various types of UV-based AOPs supported by external chemical addition such as UV/ H_2O_2 (Li

64 et al., 2015), UV/O₃ (Marquez et al., 2013), and UV/S₂O₈²⁻ (Ghauch et al., 2017) were developed for better
65 degradation of antibiotics. Recently, modified processes of VUV/UV and VUV/Fe²⁺ have been investigated
66 for the feasibility of water treatment in bench- or pilot-scale tests (Li et al., 2017; Moussavi et al., 2018c).
67 Nevertheless, the modified UV/VUV process required enormous chemical exhaustion at low pH condition
68 with relatively moderate reaction rate. Meanwhile, the effect of inorganic anions commonly present in
69 wastewaters showed various trends. Chloride (Cl⁻) and carbonate (CO₃²⁻) suppressed reaction rates of
70 UV/S₂O₈²⁻ and UV/H₂O₂ systems, whereas they elevated the degradation rates of UV/peroxymonosulfate
71 (PMS) treatment (Dhaka et al., 2018).

72 Despite the increasing popularity of UV-based AOPs supported by external chemical addition, the
73 feasibility of using chemical agents to improve the efficiency of VUV-based AOPs toward antibiotics removal
74 remains uncertain. This substantiates the need for developing technology that can effectively remove these
75 micro-contaminants under neutral pH condition with low chemical input and high efficiency in presence of
76 effecting inorganic anions. In this study, the candidates of chemical agents that can be employed for the
77 enhancement of VUV photolysis are H₂O₂ and S₂O₈²⁻, because their oxidative ability has been proven for the
78 decomposition of aqueous organics. Therefore, we aimed to examine the effects of H₂O₂ and S₂O₈²⁻ addition
79 on the degradation of various types of antibiotics (CEX, OFX, and NOF) in water under VUV irradiation in
80 comparison with UV-based processes. In view of the significant effect of halides on oxidation processes (Wu
81 et al., 2017), the single or binary presence of halides (Cl⁻ and Br⁻) on the degradation of antibiotics was also
82 examined. A three factorial Box-Behnken design was then employed to optimize the relevant parameters for
83 the degradation of OFX under VUV irradiation.

84

85 **2. Materials & Methods**

86 2.1. Chemical reagents and materials

87 All chemicals were of analytical reagent grade and solvents were of HPLC grade. Cefalexin
88 ($C_{16}H_{17}N_3O_4S$, CEX), norfloxacin ($C_{16}H_{18}FN_3O_3$, NOR), and ofloxacin ($C_{18}H_{20}FN_3O_3$, OFX) were
89 purchased from Wako Pure Chemical Industries, Ltd., Japan. The physicochemical characteristics of
90 antibiotics are summarized in Table S1. Sodium hydroxide (NaOH, 96%), sodium thiosulfate ($Na_2S_2O_3$),
91 sodium chloride (NaCl, 99%), and potassium bromide (KBr) were obtained from Uni-Chem Co., Ltd., South
92 Korea. Hydrogen peroxide (H_2O_2), potassium peroxydisulfate ($K_2S_2O_8$), acetonitrile (HPLC grade, C_2H_3N),
93 and trimethylamine (HPLC grade, $C_6H_{15}N$) were purchased from VWR Chemicals (USA), Riedel-deHaën
94 (Germany), DUKSAN (South Korea), and Alfa Aesar (USA), respectively.

95

96 2.2. Photo-oxidation experiments

97 A 300-mL (50 mm ID \times 310 mm H) tailor-made reactor with a single-layered quartz sleeve inside was
98 used as a photo-reactor coupled with a magnetic stirring apparatus. UV (254 nm) and VUV (185 nm) mercury
99 containing lamps (39 W low pressure) were applied and the irradiance of 1.3×10^{-8} Einstein's $L^{-1} s^{-1}$ was
100 measured by iodide-iodate actinometry. The schematic of the photo-reactor is shown in Fig. 1. The photolytic
101 experiments were performed at 23 ± 2 °C, and the initial pH of solution was adjusted by orthophosphoric acid
102 as needed. Appropriate amounts of stock solutions of CEX, NOF, and OFX in distilled de-ionized water
103 (DDW) were spiked into the photo-reactor containing 300 mL DDW to obtain the initial concentration of
104 antibiotics to $10 \text{ mg } L^{-1}$, which represented the concentrations of organic pollutants in antibiotics-containing
105 industrial wastewaters (Shi et al., 2017). For the implementation of modified UV-C or VUV process, a certain
106 amount of H_2O_2 or $K_2S_2O_8$ was added to the solutions and subjected to UV-C or VUV irradiation. The reactor
107 was operated with rapid mixing by a magnetic stirring apparatus at the bottom of the reactor, and each
108 photoreaction solution was stirred by intensive mixing. At each interval for sampling, a sample of 1.5 mL was
109 withdrawn from the reactor and then further oxidation reactions were immediately stopped by adding excess

110 Na₂SO₃ that can quench radicals generated by H₂O₂ or K₂S₂O₈ (García-Galán et al., 2016). Then, the sample
111 was filtered through a 0.45-µm pore-size polyvinylidene fluoride syringe filter (Whatman, USA) and
112 analyzed for the antibiotics concentrations; 30% of the experiments were randomly replicated to ensure data
113 reproducibility and reliability. The pseudo-first order kinetics model (equation 1) was used to show the kinetic
114 data of degradation of antibiotics:

$$\ln\left(\frac{C_0}{C}\right) = k_{obs}t \quad (1)$$

115 where C_0 and C represent the antibiotics concentration before reaction and at the reaction time t , respectively;
116 and k_{obs} is the observed rate constant of degradation.

117

118 2.3. Analytical methods

119 The determination of antibiotics was performed by a high-performance liquid chromatograph (HPLC)
120 equipped with an Alltech Model 426 HPLC pump and a LINEAR UV/Visible 200 absorbance detector. A
121 Pinnacle DB C18 reversed phase column (250 mm × 4.6 mm with i.d. of 5 µm) was used for chromatographic
122 separations. For the quantification of antibiotics, the mobile phase consisted of acetonitrile, water, and
123 triethylamine (18:82:3, v/v), and the solution pH value was adjusted to 3. The mobile phase was filtered
124 through a 0.2-µm pore-size polytetrafluoroethylene membrane filter (Whatman, USA) and degassed for 30
125 min. The mobile phase was pumped at a flow rate of 1 mL min⁻¹ and then 20-µL sample was injected into the
126 HPLC system. The UV/Visible detector was set at a wavelength of 261 nm, 270 nm, and 294 nm for CEX,
127 NOF, and OFX, respectively. The solution pH was measured by a PHS-3C digital pH meter.

128

129 2.4. Box-Behnken Experimental Design

130 Responsible surface method (RSM) is a statistical approach to determine the significance and effects of

131 independent variables (input variables) as well as to optimize the responses (output variables) in experimental
132 process. The RSM was applied to investigate the effects of three variables that have been identified as main
133 parameters from previous studies for organic removal by UV/VUV-based AOPs: H₂O₂ concentration (0-1
134 mM), K₂S₂O₈ concentration (0-1 mM), and solution pH (5-9) on the degradation kinetics of OFX in this work.
135 For the investigation on the effects of three variables, 17 experiments designed by Box-Behnken were
136 conducted, and the pseudo-first-order rate constant (k_{obs}) of OFX degradation by VUV-based processes during
137 1.5 min was estimated as the response factor. The second-order quadratic polynomial equation was used to
138 determine the interaction effects between the variables, and the predicted response can be quantitatively
139 described as a quadratic function of three variables (Table S2). The equation can be expressed as follows:

$$140 Y = \beta_0 + \beta_1 X_1 + \beta_2 X_2 + \beta_3 X_3 + \beta_{12} X_1 X_2 + \beta_{13} X_1 X_3 + \beta_{23} X_2 X_3 + \beta_{11} X_1^2 + \beta_{22} X_2^2 + \beta_{33} X_3^2 \quad (2)$$

141 where solution pH is X₁, initial concentration of H₂O₂ is X₂, and initial concentration of K₂S₂O₈ is X₃. Y is the
142 estimated response (k_{obs} value of OFX degradation); X₁, X₂, and X₃ are independent variables; β_0 is the
143 intercept; $\beta_1, \beta_2,$ and β_3 are liner coefficients; $\beta_{12}, \beta_{13},$ and β_{23} are squared coefficients;
144 $\beta_{11}, \beta_{22},$ and β_{33} are quadratic coefficients. The accuracy of the proposed polynomial model was
145 examined by analysis of variance (ANOVA). The three real levels and coded levels are presented in Table S3.

146

147 **3. Results & Discussion**

148 3.1. Degradation of OFX, NOF, and CEX by UV- and VUV based processes

149 The photolytic degradation experiments of antibiotics (OFX, NOF, and CEX) by UV- or VUV-based
150 processes were conducted, and the degradation kinetics data and k_{obs} values are presented in Fig. 2. Without
151 excitation of light source, only 14-43% of OFX was degraded during 30-min reaction when either H₂O₂ or
152 K₂S₂O₈ was added only (Fig. S1), despite the oxidative capacities of H₂O₂ ($E^\circ = 1.8 \text{ V}$) (Fuku et al., 2016) and

153 $S_2O_8^{2-}$ ($E^\circ = 2.01$ V) (Matzek and Carter, 2016). The values of k_{obs} for CEX degradation rate under
154 homogeneous UV and VUV processes reached approximately 1.0 min^{-1} , while those of NOF and OFX were
155 slow at the same conditions with the values of k_{obs} lower than 0.25 min^{-1} . Direct photolysis might be the main
156 degradation mechanism for effective CEX degradation. However, the degradation rate of OFX was
157 comparatively low in the homogeneous UV and VUV processes, with 40% and 97% removal of OFX for 30
158 min, respectively. This observation suggests that fluoroquinolone antibiotics (FQs) are more resistant to the
159 photolysis compared to sulfur-containing antibiotics (e.g., CEX). As a result, an individual process by either
160 chemical agents or irradiation alone was not sufficient to remove the FQs from water.

161 The addition of chemical agents (H_2O_2 or $K_2S_2O_8$) remarkably increased the degradation rates of the three
162 antibiotics, and the effects were more pronounced for FQs degradation under VUV irradiation in the presence
163 of H_2O_2 or $K_2S_2O_8$ individually. As illustrated in Fig. 2a&b, the degradation efficiencies of OFX and NOF
164 dramatically increased in the following order: $UV < VUV < UV/H_2O_2 < UV/K_2S_2O_8 < VUV/H_2O_2 <$
165 $VUV/K_2S_2O_8$ (0.04 to 2.05 min^{-1}), indicating that UV or VUV irradiation is more compatible with $K_2S_2O_8$
166 addition than H_2O_2 addition. On the contrary, the degradation of CEX showed the opposite tendency. The
167 addition of H_2O_2 resulted in slightly faster degradation of CEX under UV or VUV irradiation than $K_2S_2O_8$
168 addition (Fig. 2c).

169 The higher CEX degradation efficiency via UV/VUV with H_2O_2 addition compared to that with $K_2S_2O_8$
170 could be justified by the relatively slow reaction of β -lactams rings in CEX with $SO_4^{\cdot-}$ than $\cdot OH$ (He et al.,
171 2016). The accelerated degradation rate after H_2O_2 addition in the presence of UV light might result from a
172 larger amount of generated $\cdot OH$ during photolysis (*viz.* $H_2O_2 + UV_{254} \rightarrow 2\cdot OH$) (Mondal et al., 2018), which
173 apparently could facilitate the faster degradation of CEX. By contrast, more degradation of FQs in the
174 presence of $K_2S_2O_8$ under UV or VUV irradiation compared to the case in the presence of H_2O_2 could be
175 explained by the cleavage of C-F bonds of the FQs via defluorination, hydroxylation of the FQs through self-

176 sensitized photo-process, and piperazine ring cleavage by the attack of $\cdot\text{OH}/\text{SO}_4^{\cdot-}$ radicals (Ao et al., 2018).
177 Meanwhile, Jin et al. (2018a) proposed that free radicals of $\text{SO}_4^{\cdot-}$ and $\cdot\text{OH}$ could attack active sites of
178 antibiotics (*e.g.*, aromatic rings and olefinic double bonds) *via* one electron transfer producing carbon-centered
179 radical cations, which further transformed into the OH adducts after hydrolysis. Moreover, hydrogen
180 abstraction induced hydroxyl-organic radical that was eventually mineralized into smaller organic molecules,
181 CO_2 , and H_2O (Jin et al., 2018b; Wang et al., 2018). The simultaneous, multi-pathway mediated FQs
182 degradation in UV/ $\text{K}_2\text{S}_2\text{O}_8$ could contribute to the enhancement of the reaction rate.

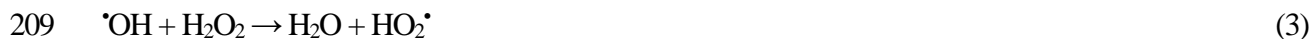
183 One interesting observation is the synergistic effect arising from the combination of chemical addition and
184 VUV irradiation, which accounted for the fastest degradation rate of FQs. The k_{obs} values of VUV/ H_2O_2 and
185 VUV/ $\text{K}_2\text{S}_2\text{O}_8$ for OFX and NOF were comparable to the k_{obs} of CEX at the same condition ($> 2.0 \text{ min}^{-1}$),
186 which can be attributed to the generation of abundant reactive radical species of $\cdot\text{OH}/\text{SO}_4^{\cdot-}$ in the modified
187 VUV processes (Moussavi et al., 2018a). The VUV/ H_2O_2 process was reported to allow better degradation
188 of clofibric acid (over 99% removal efficiency) compared to that by either UV/ H_2O_2 or VUV alone (Li et al.,
189 2011). Recently, Moussavi et al. (2018a) revealed the enhancement of degradation of cyanide in industrial
190 wastewater when employing VUV/ $\text{K}_2\text{S}_2\text{O}_8$ process, possibly due to the simultaneous production of reactive
191 radical species in a short period of time.

192 Considering less degradation of OFX and NOF by $\cdot\text{OH}$ generated from water photolysis in the presence
193 of modified UV processes (Fig. 2a&b), the effectiveness of chemical addition might be further amplified
194 under VUV irradiation. Moreover, $\text{S}_2\text{O}_8^{2-}$ activation can be largely affected by the wavelength of light
195 irradiation. The relatively fast activation by 185 nm light irradiation compared to that by 254 nm light
196 irradiation has been validated with the corresponding loss rate of $\text{S}_2\text{O}_8^{2-}$ at different wavelengths (185 nm and
197 254 nm) (An et al., 2015).

198

199 3.2. Comparison of OFX degradation in VUV/H₂O₂ and VUV/K₂S₂O₈

200 To get more insights into the effects of chemical agents on the degradation of antibiotic under VUV
201 irradiation, the degradation kinetics of OFX at different concentrations of H₂O₂ and K₂S₂O₈ (0.25-5 mM)
202 were investigated and the results are shown in Fig. 3a and Fig. 3b. The degradation rate of OFX increased
203 gradually with the increasing concentration of H₂O₂ from 0.25 to 1 mM under VUV irradiation, with the
204 highest k_{obs} of 2.8 min⁻¹ at 1 mM H₂O₂ (Fig. 3a). This observation suggests that H₂O₂ activated by VUV
205 irradiation could generate more reactive species thus leading to promoted degradation of OFX. However,
206 further addition of H₂O₂ over 1 mM slightly retarded the degradation rate, possibly due to the scavenged [•]OH
207 through a chain termination reaction (equations 3 and 4) at a high dosage of H₂O₂ (Gu et al., 2012), thereby
208 decreasing the overall degradation capacity.



211 The degradation of OFX in VUV/K₂S₂O₈ process was more effective than that in VUV/H₂O₂ process at the
212 same concentration, which can be explained by the wider gap of redox potential between OFX and [•]OH (E°
213 = 1.8-2.7 V) than SO₄^{•-} ($E^\circ = 2.5-3.1$ V) (O'Connor et al., 2018). Increasing the concentration of K₂S₂O₈
214 remarkably boosted the degradation rate of OFX (Fig. 3b), i.e., the k_{obs} value increased from 1.70 to 9.05 min⁻¹
215 with increasing K₂S₂O₈ concentration from 0.25 to 5 mM. This observation implies the simultaneous
216 production of [•]OH/SO₄^{•-} via a variety of reaction pathways (*viz.* H₂O + VUV_{185 nm} → [•]OH + H[•]; H₂O + VUV₁₈₅
217 nm → [•]OH + H[•] + e_{aq}⁻; S₂O₈²⁻ + VUV_{185 nm} → 2SO₄^{•-}; S₂O₈²⁻ + e_{aq}⁻ → SO₄²⁻ + SO₄^{•-}) without the critical
218 scavenging reaction that eliminates the reactive radicals (Moussavi et al., 2018a). Moreover, this rate
219 enhancement was probably associated with the continuous activation of S₂O₈²⁻ by [•]OH and e_{aq}⁻ generated
220 from VUV photolysis so that a large amount of SO₄^{•-} with a high redox potential could be produced. However,
221 further addition of K₂S₂O₈ over 3 mM did not increase the degradation rate, because the restrained reaction

222 of $\text{SO}_4^{\cdot-}$ by either H_2O or $\text{S}_2\text{O}_8^{2-}$ (*viz.*, $\text{SO}_4^{\cdot-} + \text{H}_2\text{O} \rightarrow \text{HSO}_4^- + \cdot\text{OH}$ or $\text{SO}_4^{\cdot-} + \text{S}_2\text{O}_8^{2-} \rightarrow \text{SO}_4^{2-} + \text{S}_2\text{O}_8^{\cdot-}$)
223 produced less reactive radicals due to the excessive concentration of $\text{SO}_4^{\cdot-}$ (Yu et al., 2004). Therefore, the
224 results indicate that, under VUV irradiation, $\text{K}_2\text{S}_2\text{O}_8$ was more effective than H_2O_2 for enhancing the
225 degradation rate of FQs, especially when a high dose of chemical agent was applied.

226 The degradation efficiency of OFX observed in the VUV/ $\text{K}_2\text{S}_2\text{O}_8$ process was compared with the
227 processes reported in the literature although the experimental conditions were different from each other, and
228 the result are summarized in Table 2. For example, modified mesoporous iron oxide catalyzed H_2O_2 oxidation
229 process needed 50-min reaction time to completely degrade 12 mg L^{-1} OFX at pH 6.4 (Tian et al., 2017),
230 which implies the slow degradation kinetics rate of OFX without irradiation. The process of polyvinylidene
231 fluoride membrane soaked with 42 mM $\text{Na}_2\text{S}_2\text{O}_8$ solution only exhibited 54% removal of 5 mg L^{-1} OFX in
232 30 min under UV irradiation at 395 nm (Wang et al., 2017). The UV/ H_2O_2 process applied to wastewater
233 containing 9 mM H_2O_2 rapidly degraded 0.5 mg L^{-1} OFX in 8.5 min (Urbano et al., 2017), but the complete
234 degradation of 10 mg L^{-1} OFX needed longer reaction time of 30 min in the presence of 7.94 mM H_2O_2 under
235 UV irradiation at 254 nm (Lin et al., 2016). Compared to the above processes, VUV/ $\text{K}_2\text{S}_2\text{O}_8$ in this study
236 showed relatively fast degradation of OFX in a very short period of time, i.e., almost 100% removal within 2
237 min.

238 The effect of solution pH on the degradation rate of OFX by VUV/ H_2O_2 and VUV/ $\text{K}_2\text{S}_2\text{O}_8$ was
239 investigated and the results are shown in Fig. 3c and Fig. 3d. The overall degradation rates of OFX were
240 highly dependent on the solution pH in both VUV/ H_2O_2 and VUV/ $\text{K}_2\text{S}_2\text{O}_8$ systems. Basically, an increase of
241 solution pH resulted in the decline of the degradation rate. This was because the formation of negatively
242 charged OFX molecules under alkaline condition ($\text{pK}_{\text{a}1} = 6.05$ and $\text{pK}_{\text{a}2} = 8.11$) reduced the degradation rate
243 in both processes where $\cdot\text{OH}$ was more reactive to non-ionic molecules (Liao et al., 2016). The decreasing
244 redox potential of $\cdot\text{OH}$ with increasing pH might be another reason for the lower degradation rate of OFX

245 (Moussavi et al., 2018b). Considering that the predominant reactive species were $\cdot\text{OH}$ in VUV/ H_2O_2 system,
246 the OFX degradation associated with $\cdot\text{OH}$ could render the VUV/ H_2O_2 irradiation sensitive to the increase of
247 solution pH. The pronounced decline of the degradation rate was apparent at pH 11 (Fig. 3c), which was
248 ascribable to the active self-decomposition of H_2O_2 (*viz.* $2\text{H}_2\text{O}_2 \rightarrow \text{H}_2\text{O} + \text{O}_2$). The elevation of solution pH
249 gradually decreased the degradation rate of OFX (Fig. 3d) in VUV/ $\text{K}_2\text{S}_2\text{O}_8$ system, which could be attributed
250 to the consumption of $\text{SO}_4^{\cdot-}$ by $\cdot\text{OH}$ (*viz.* $\text{SO}_4^{\cdot-} + \text{OH}^- \rightarrow \cdot\text{OH} + \text{SO}_4^{2-}$) forming less reactive radical (Guan
251 et al., 2011). The accelerated degradation rate was observed at low pH in VUV/ $\text{K}_2\text{S}_2\text{O}_8$ process with the k_{obs}
252 value of 1.93 min^{-1} at pH 3 (Fig. 3d). This observation suggests that the decomposition of $\text{S}_2\text{O}_8^{2-}$ can be
253 catalytically accelerated by the protonation reaction of $\text{S}_2\text{O}_8^{2-}$ (*viz.* $\text{S}_2\text{O}_8^{2-} + \text{H}^+ \rightarrow \text{HS}_2\text{O}_8^-$; $\text{HS}_2\text{O}_8^- \rightarrow 2\text{SO}_4^{\cdot-}$
254 + H^+) (House, 1962). Interestingly, the highest OFX removal rate was achieved in both VUV/ H_2O_2 and
255 VUV/ $\text{K}_2\text{S}_2\text{O}_8$ processes when the solution pH was not adjusted (7.5-8.0). This phenomenon could be
256 associated with the greater resistance of cationic form of OFX at low pH (< 6.05) to the electrophilic attack of
257 radicals (Li et al., 2017).

258

259 3.3. Effects of halide ions on degradation of antibiotics

260 To examine how the single or binary existence of halides (*i.e.*, chloride and bromide) influences the
261 degradation of antibiotics by VUV photolysis, the removal of NOF and CEX in presence of halide ions under
262 VUV irradiation was investigated and the results are shown in Fig. 4. Following the similar level of halide
263 ions selected in relevant studies (Li et al., 2015), the concentration of Cl^- ions ranged from 0.03 to 0.2 M while
264 the low concentration range of 0.05-0.25 mM was chosen for Br^- ions. The degradation rates of CEX and NOF
265 by VUV photolysis were 0.967 and 0.266 min^{-1} in the absence of Cl^- and Br^- , respectively. Meanwhile, the
266 addition of 0.03 M Cl^- contributed to a slight enhancement in the degradation rate, probably because the
267 chlorine radical (Cl^\cdot) and e_{aq}^- were generated under these conditions (*viz.* $\text{Cl}^- + \text{VUV}_{185 \text{ nm}} \rightarrow \text{Cl}^\cdot + e_{\text{aq}}^-$)

268 facilitating the degradation of CEX (Furati and Mohseni, 2018). However, further increasing Cl^-
269 concentration from 0.03 to 0.2 M lowered the k_{obs} values of CEX and NOF from 1.02 and 0.42 min^{-1} to 0.85
270 and 0.32 min^{-1} , respectively. This observation could be attributed to the scavenging of $\cdot\text{OH}$ caused by the
271 reaction between Cl^- and $\cdot\text{OH}$ at high levels of Cl^- (*i.e.*, saline water) (Grebel et al., 2010), thereby decreasing
272 the overall degradation rate. The impeded degradation of CEX in the presence of Br^- is because of the $\cdot\text{OH}$
273 consumption by Br^- in VUV photolysis forming another reactive radical (*viz.* $\text{Br}^- + \cdot\text{OH} \rightarrow \text{BrOH}^\cdot$) (Cheng
274 et al., 2018).

275 Contrasting to the inhibition of CEX degradation by the Br^- addition, the k_{obs} value for NOF degradation
276 gradually increased to 0.395 min^{-1} with Br^- concentration increasing from 0.05 to 0.25 mM. The unexpected
277 enhancement of NOF degradation by Br^- addition was attributable to the electron-rich moieties of FQs with
278 higher susceptibility toward reactive halogen species (RHS) radicals (Cheng et al., 2018). Thus, the
279 participation of RHS radicals in the FQs degradation could offset the efficiency loss caused by $\cdot\text{OH}$
280 scavenging (Grebel et al., 2010). Compared with the presence of single halide ions, the co-existence of
281 chloride and bromide slightly increased the k_{obs} values under VUV irradiation, which was likely due to the
282 conversion of non-selective $\cdot\text{OH}$ to selective RHS radicals (primarily ClBr^\cdot) (Heeb et al., 2014). As a result,
283 owing to the more unsaturated bonds readily to be attacked by $\cdot\text{OH}$, the degradation of FQs was much more
284 susceptible to the presence of halides in VUV photolysis than CEX.

285 The effect of halides on the degradation of OFX in VUV/ H_2O_2 and VUV/ $\text{K}_2\text{S}_2\text{O}_8$ processes was
286 examined and the results are shown in Fig. 5. As illustrated in Fig. 5a, the presence of Cl^- showed no obvious
287 impact on OFX degradation in VUV/ H_2O_2 and VUV/ $\text{K}_2\text{S}_2\text{O}_8$ processes. This observation could result from
288 the dynamic equilibrium between the formation and the dissociation of ClOH^\cdot (*viz.* $\text{Cl}^- + \cdot\text{OH} \leftrightarrow \text{ClOH}^\cdot$)
289 ($k = 4.3 \times 10^9 \text{ M}^{-1} \text{ s}^{-1}$) such that the level of $\cdot\text{OH}$ could be stabilized (Yin et al., 2018). For VUV/ $\text{K}_2\text{S}_2\text{O}_8$
290 process, the addition of Br^- at low level (0.05 mM) promoted the degradation rate of OFX, even though the

291 halide ions have been well-known as primary scavengers of $\cdot\text{OH}$ and $\text{SO}_4^{\cdot-}$ (equations 5-9) (Yang et al., 2014).



297 Interestingly, the co-existence of Cl^- and Br^- facilitated the highest degradation of OFX in both VUV/ H_2O_2

298 and VUV/ $\text{K}_2\text{S}_2\text{O}_8$ processes (Fig. 5b). As reported by Li et al. (2015), $\text{ClBr}^{\cdot-}$ possibly dominated the OFX

299 degradation via the following reactions (equations 10-14),



305 As a result, a variety of radical species including Br-containing radicals (especially Br^\bullet , $\text{Br}_2^{\cdot-}$, and $\text{ClBr}^{\cdot-}$),

306 non-radicals (HOX , X_2 , and X_3^-), and RHS radicals were formed in the presence of halides and possibly

307 rendered the faster degradation of the antibiotics.

308

309 3.4. Optimization of chemical addition in VUV system based on RSM

310 The Box-Behnken experimental design consisted of 17 experiments with three independent variables:

311 (1) solution pH, (2) initial concentration of H_2O_2 , and (3) initial concentration of $\text{K}_2\text{S}_2\text{O}_8$. The k_{obs} values of

312 OFX degradation within 1.5-min reaction from the 17 experiments are shown in Table 2. Multiple regression

313 analysis was employed to identify the relationship between the response and three variables. The results
314 indicate that the model-predicted responses were in good agreement with the experimental data. The
315 polynomial second order analysis (equation 15) illustrated the relationship between the response and the three
316 variables,

$$317 \quad Y = 2.37 - 0.071X_1 + 0.59X_2 + 0.69X_3 + 0.0084X_1X_2 - 0.055X_1X_3 - 0.18X_2X_3 - 0.25X_1^2 - 0.33X_2^2 \quad (15)$$

318 where Y is the predicted k_{obs} value of OFX degradation within 1.5-min reaction, and the X_1 , X_2 , and X_3 are
319 the solution pH and initial concentrations of H_2O_2 and $\text{K}_2\text{S}_2\text{O}_8$, respectively.

320 The ANOVA analysis of the above model is provided in Table S4, and the F-value of 23.2 implied the
321 model was accurate. The probability value (P) was employed to identify the significance of terms, which are
322 considered as significant to the predicted response when $P < 0.05$. X_2 , X_3 , X_{12} , X_{22} , and X_{32} were significant
323 ($P < 0.05$) for predicted response, while X_1 , X_1X_2 , X_1X_3 , and X_2X_3 were insignificant ($P > 0.1$) model terms.
324 The “Lack of Fit F-value” of 3.12 suggested the lack of fit was not significant relative to the pure error, which
325 had a 15.0% chance of noise interruption and was fitted well by the model.

326 The determination coefficient (R^2) was used to confirm the suitability of the quadratic model. The value
327 of adjusted R^2 was calculated as 0.926 (Fig. S1a). The standard error design of model H_2O_2 dose versus
328 solution pH at fixed $\text{K}_2\text{S}_2\text{O}_8$ dose at central level (Fig. S1b) indicated that the design space could be directed
329 by the proposed model. The data of Studentized residuals were distributed at either side of line homogeneously,
330 indicating a satisfactory suitability of the proposed quadratic model in this work ($R^2 = 0.968$) (Fig S1c). To
331 obtain the optimal conditions for the removal of OFX (Y), the 3D response surface plots were generated (Fig.
332 6) and used to investigate the influence of any two independent variables on the measured responses with one
333 variable fixed at the central level.

334 Although solution pH was not an influencing parameter on the OFX removal in water, better removal
335 efficiency was achieved in acidic solution. Alkaline condition was unfavorable for the antibiotic degradation

336 with $K_2S_2O_8$ addition. The Y increased with the increasing H_2O_2 and $K_2S_2O_8$ concentrations until Y reached
337 the highest value. According to the optimization analysis (Table 2), the optimal value of each concentration
338 for Y was both 1 mM when a single chemical agent was applied. As demonstrated in Section 3.2, however,
339 increasing the single amount of H_2O_2 and $K_2S_2O_8$ has a limit in enhancing the degradation rate. As UV/ H_2O_2
340 process could be enhanced at a low H_2O_2 concentration by the addition of $S_2O_8^{2-}$ due to more generation of
341 $SO_4^{\bullet-}$ (Chu et al., 2006), it is worth simulating if the co-use of H_2O_2 and $K_2S_2O_8$ would be effective for the
342 degradation of OFX under VUV irradiation before experimental validation. As a result, the optimal values of
343 H_2O_2 and $K_2S_2O_8$ concentrations were found to be 0.82 and 0.97 mM under the co-existence condition. Given
344 the simulation results, combinations of H_2O_2 and $K_2S_2O_8$ in VUV process should be examined in an empirical
345 way in order to maximize and accelerate the degradation of antibiotics in further study.

346

347 **4. Implications for industrial applications**

348 In a previous study, a pilot-scale UV/ H_2O_2 system has been successfully run for over two months to remove
349 15 trace organic chemicals from the effluent of municipal wastewater treatment plant (Miklos et al., 2018).
350 Nevertheless, when considering the known disadvantages of H_2O_2 (e.g., corrosiveness of process water and
351 self-disintegration loss during its transport), the use of $K_2S_2O_8$ is preferable for practical application. Moreover,
352 for industrial application, it is very difficult to maintain the solution pH at 2-3 and after treatment the
353 wastewater has to be neutralized before effluent discharge. The current study shows that the removal of
354 antibiotics from waters can be achieved at neutral pH condition. Besides, previous research indicated that the
355 VUV/ $S_2O_8^{2-}$ system was a more proficient and economical ($\$6.26 /m^3$ water) process for the removal of
356 organics than other AOP (e.g., heat-activated $S_2O_8^{2-}$, Fenton, photo-Fenton, UV/ H_2O_2 , and UV/PMS)
357 methods (Dhaka et al., 2018). Based on the overall results, VUV/ $K_2S_2O_8$ process appears to be a promising
358 method for the degradation of CEX, OFX, and NOF in saline antibiotics-containing wastewaters.

359

360 **5. Conclusions**

361 The degradation rates of CEX, NOF, and OFX via various UV- and VUV-based processes were evaluated
362 and compared. The degradation rates of OFX and NOF (fluoroquinolones) by the sole application of UV or
363 VUV were inferior to that of CEX. The $K_2S_2O_8/H_2O_2$ assisted photolysis improved the antibiotics degradation,
364 while $K_2S_2O_8$ was more effective than H_2O_2 with the observed rate constant (k_{obs}) ($2.05-0.04 \text{ min}^{-1}$) decreasing
365 in the following order: $VUV/K_2S_2O_8 > VUV/H_2O_2 > UV/K_2S_2O_8 > UV/H_2O_2 > VUV > UV$. The adverse
366 effect (*i.e.*, $\cdot OH$ loss by scavenging reaction) due to the excess use of H_2O_2 was not observed in $VUV/K_2S_2O_8$
367 process. The single presence of halide ions (Cl^- and Br^-) exhibited a negative impact on the NOF degradation
368 by VUV photolysis, which was mitigated by co-existence of Cl^- and Br^- . However, the co-existence of
369 halides accelerated the OFX degradation rate in VUV/H_2O_2 and $VUV/K_2S_2O_8$ processes due to the generation
370 of abundant reactive radicals. The concentrations of H_2O_2 and $K_2S_2O_8$ were evaluated as critical variables and
371 optimized for maximizing the OFX removal via RSM. This proposed AOP has advantages of less chemical
372 input, fast kinetics, no sludge production, and high degree of mineralization, which can be considered as a
373 cleaner treatment option for the elimination of recalcitrant pollutants in future work.

374

375 **Acknowledgement**

376 The authors appreciate the financial support from the Hong Kong Research Grants Council (PolyU 15217818
377 and E-PolyU503/17) for this study.

378

379 **References**

380 Ahmed, M.J. and Theydan, S.K., 2014. Fluoroquinolones antibiotics adsorption onto microporous activated
381 carbon from lignocellulosic biomass by microwave pyrolysis. J. Taiwan Inst. Chem. E. 45, 219-226.

382 An, D., Westerhoff, P., Zheng, M., Wu, M., Yang, Y., Chiu, C.A., 2015. UV-activated persulfate oxidation and
383 regeneration of NOM-saturated granular activated carbon. *Water Res.* 73, 304-310.

384 Ao, X., Liu, W., Sun, W., Cai, M., Ye, Z., Yang, C., Lu, Z.D., Li, C., 2018. Medium pressure UV-activated
385 peroxymonosulfate for ciprofloxacin degradation: Kinetics, mechanism, and genotoxicity. *Chem. Eng.*
386 *J.* 345, 87-97.

387 Cheng, S.S., Zhang, X., Yang, X., Shang, C., Song, W., Fang, J., Pan, Y., 2018. The multiple role of bromide
388 ion in PPCPs degradation under UV/chlorine treatment. *Environ. Sci. Technol.* 52, 1806-1816.

389 Chu, W., Lau, T.K., Fung, S.C., 2006. Effects of combined and sequential addition of dual oxidants
390 ($\text{H}_2\text{O}_2/\text{S}_2\text{O}_8^{2-}$) on the aqueous carbofuran photodegradation. *J. Agr. Food Chem.* 54, 10047-10052.

391 Copete-Pertuz, L.S., Plácido, J., Serna-Galvis, E.A., Torres-Palma, R.A., Mora, A., 2018. Elimination of
392 Isoxazolyl-Penicillins antibiotics in waters by the ligninolytic native Colombian strain *Leptosphaerulina*
393 *sp* considerations on biodegradation process and antimicrobial activity removal. *Sci. Total Environ.* 630,
394 1195-1204.

395 Dhaka, S., Kumar, R., Lee, S.H., Kurade, M.B., Jeon, B.H., 2018. Degradation of ethyl paraben in aqueous
396 medium using advanced oxidation processes: Efficiency evaluation of UV-C supported oxidants. *J.*
397 *Clean. Prod.* 180, 505-513.

398 Fuku, K., Miyase, Y., Miseki, Y., Gunji, T., Sayama, K., 2016. Enhanced oxidative hydrogen peroxide
399 production on conducting glass anodes modified with metal oxides. *Chemistryselect* 1, 5721-5726.

400 Furatian, L. and Mohsenr, M., 2018. Influence of major anions on the 185 nm advanced oxidation process -
401 Sulphate, bicarbonate, and chloride. *Chemosphere* 201, 503-510.

402 García-Galán, M.J., Anfruns, A., Gonzalez-Olmos, R., Rodríguez-Mozaz, S., Comas, J., 2016. UV/ H_2O_2
403 degradation of the antidepressants venlafaxine and O-desmethylvenlafaxine: Elucidation of their
404 transformation pathway and environmental fate. *J. Hazard. Mater.* 311, 70-80.

405 Ghauch, A., Baalbaki, A., Amasha, M., El Asmar, R., Tantawi, O., 2017. Contribution of persulfate in UV-
406 254 nm activated systems for complete degradation of chloramphenicol antibiotic in water. *Chem. Eng.*
407 *J.* 317, 1012-1025.

408 Grebel, J.E., Pignatello, J.J., Mitch, W.A., 2010. Effect of halide ions and carbonates on organic contaminant
409 degradation by hydroxyl radical-based advanced oxidation processes in saline waters. *Environ. Sci.*
410 *Technol.* 44, 6822-6828.

411 Guan, Y.H., Ma, J., Li, X.C., Fang, J.Y., Chen, L.W., 2011. Influence of pH on the formation of sulfate and
412 hydroxyl radicals in the UV/peroxymonosulfate system. *Environ. Sci. Technol.* 45, 9308-9314.

413 Guo, Y., Tsang, D.C.W, Zhang, X., Yang, X., 2018. Cu(II)-catalyzed degradation of ampicillin: effect of pH
414 and dissolved oxygen. *Environ. Sci. Pollut. Res.* 25, 4279-4288.

415 Gu, X., Lu, S., Qiu, Z., Sui, Q., Miao, Z., Lin, K., Liu, Y., Luo, Q., 2012. Comparison of photodegradation
416 performance of 1, 1, 1-trichloroethane in aqueous solution with the addition of H₂O₂ or S₂O₈²⁻ oxidants.
417 *Ind. Eng. Chem. Res.* 51, 7196-7204.

418 Heeb, M.B., Criquet, J., Zimmermann-Steffens, S.G., Von Gunten, U., 2014. Oxidative treatment of bromide-
419 containing waters: Formation of bromine and its reactions with inorganic and organic compounds - A
420 critical review. *Water Res.* 48, 15-42.

421 He, X., Mezyk, S.P., Michael, I., Fatta-Kassinos, D., Dionysiou, D.D., 2014. Degradation kinetics and
422 mechanism of beta-lactam antibiotics by the activation of H₂O₂ and Na₂S₂O₈ under UV-254 nm
423 irradiation. *J. Hazard. Mater.* 279, 375-383.

424 Hou, D.Y, Qi, S., Zhao, B., Rigby, M., O'Connor, D., 2017. Incorporating life cycle assessment with health
425 risk assessment to select the 'greenest' cleanup level for Pb contaminated soil. *J. Clean. Prod.* 162, 1157-
426 1168.

427 House, D.A., 1962. Kinetics and mechanism of oxidations by peroxydisulfate. *Chem. Rev.* 62, 185-203.

428 Jin, J., Feng, T., Gao, R., Ma, Y., Wang, W., Zhou, Q., Li, A., 2018. Ultrahigh selective adsorption of
429 zwitterionic PPCPs both in the absence and presence of humic acid: Performance and mechanism. *J.*
430 *Hazard. Mater.* 348, 117-124.

431 Jin, Q., Wang, H., Hu, C., Chen, Z., Wang, X., 2018a. Effects of NOM on the degradation of chloramphenicol
432 by UV/H₂O₂ and the characteristics of degradation products. *Sep. Purif. Technol.* 191, 108-115.

433 Jin, Q., Zhang, S., Wen, T., Wang, J., Gu, P., Zhao, G., Wang, X., Chen, Z., Hayat, T., Wang, X., 2018b.
434 Simultaneous adsorption and oxidative degradation of Bisphenol A by zero-valent iron/iron carbide
435 nanoparticles encapsulated in N-doped carbon matrix. *Environ. Pollut.* 243, 218-227.

436 Kosma, C.I., Lambropoulou, D.A., Albanis, T.A., 2015. Comprehensive study of the antidiabetic drug
437 metformin and its transformation product guanylyurea in Greek wastewaters. *Water Res.* 70, 436-448.

438 Lan, Y., Coetsier, C., Causserand, C., Serrano, K.G., 2017. On the role of salts for the treatment of wastewaters
439 containing pharmaceuticals by electrochemical oxidation using a boron doped diamond anode.
440 *Electrochim. Acta.* 231, 309-318.

441 Leung, H.W., Minh, T.B., Murphy, M.B., Lam, J.C.W., So, M.K., Martin, M., Lam, P.K.S., Richardson, B.J.,
442 2012. Distribution, fate and risk assessment of antibiotics in sewage treatment plants in Hong Kong,
443 South China. *Environ. Int.* 42, 1-9.

444 Liao, Q.N., Ji, F., Li, J. C., Zhan, X., Hu, Z.H., 2016. Decomposition and mineralization of sulfaquinoxaline
445 sodium during UV/H₂O₂ oxidation processes. *Chem. Eng. J.* 284, 494-502.

446 Li, M., Wang, C., Yau, M., Bolton, J.R., Qiang, Z., 2017. Sulfamethazine degradation in water by the
447 VUV/UV process: Kinetics, mechanism and antibacterial activity determination based on a mini-fluidic
448 VUV/UV photoreaction system. *Water Res.* 108, 348-355.

449 Lin, C.C., Lin, H.Y., Hsu, L.J., 2016. Degradation of ofloxacin using UV/H₂O₂ process in a large photoreactor.
450 *Sep. Purif. Technol.* 168, 57-61.

451 Li, W., Lu, S., Qiu, Z., Lin, K., 2011. UV and VUV photolysis vs. UV/H₂O₂ and VUV/H₂O₂ treatment for
452 removal of clofibric acid from aqueous solution. *Environ. Technol.* 32, 1063-1071.

453 Li, Y., Song, W., Fu, W., Tsang, D.C.W., Yang, X., 2015. The roles of halides in the acetaminophen
454 degradation by UV/H₂O₂ treatment: Kinetics, mechanisms, and products analysis. *Chem. Eng. J.* 271,
455 214-222.

456 Lofrano, G., Libralato, G., Casaburi, A., Siciliano, A., Iannece, P., Guida, M., Pucci, L., Dentice, E.F.,
457 Carotenuto, M., 2018. Municipal wastewater spiramycin removal by conventional treatments and
458 heterogeneous photocatalysis. *Sci. Total Environ.* 624, 461-469.

459 MacDonald, M.J., Cho, D.W., Iris, K.M., Tsang, D.C.W., Yip, A.C., 2018. Photo-Fenton abatement of
460 aqueous organics using metal-organic frameworks: An advancement from benchmark zeolite. *Sci. Total*
461 *Environ.* 644, 389-397.

462 Márquez, G., Rodríguez, E.M., Beltrán, F.J., Álvarez, P.M., 2013. Determination of rate constants for
463 ozonation of ofloxacin in aqueous solution. *Ozone-Sci. Eng.* 35, 186-195.

464 Matzek, L.W. and Carter, K.E., 2016. Activated persulfate for organic chemical degradation: A review.
465 *Chemosphere.* 151, 178-188.

466 Miklos, D.B., Hartl, R., Michel, P., Linden, K.G., Drewes, J.E., Hübner, U., 2018. UV/H₂O₂ process stability
467 and pilot-scale validation for trace organic chemical removal from wastewater treatment plant effluents.
468 *Water Res.* 136, 169-179.

469 Mondal, S.K., Saha, A.K., Sinha, A., 2018. Removal of ciprofloxacin using modified advanced oxidation
470 processes: Kinetics, pathways and process optimization. *J. Clean. Prod.* 171, 1203-1214.

471 Moussavi, G. and Shekoohiyan, S., 2016. Simultaneous nitrate reduction and acetaminophen oxidation using
472 the continuous-flow chemical-less VUV process as an integrated advanced oxidation and reduction
473 process. *J. Hazard. Mater.* 318, 329-338.

474 Moussavi, G., Pourakbar, M., Aghayani, E., Mahdavianpour, M., 2018a. Investigating the aerated VUV/PS
475 process simultaneously generating hydroxyl and sulfate radicals for the oxidation of cyanide in aqueous
476 solution and industrial wastewater. *Chem. Eng. J.* 350, 673-680.

477 Moussavi, G., Pourakbar, M., Shekoohiyan, S., Satari, M., 2018b. The photochemical decomposition and
478 detoxification of bisphenol A in the VUV/H₂O₂ process: Degradation, mineralization, and cytotoxicity.
479 *Chem. Eng. J.* 331, 755-764.

480 Moussavi, G., Rezaei, M., Pourakbar, M., 2018c. Comparing VUV and VUV/Fe²⁺ processes for
481 decomposition of cloxacillin antibiotic: Degradation rate and pathways, mineralization and by-product
482 analysis. *Chem. Eng. J.* 332, 140-149.

483 O'Connor, D., Hou, D., Ok, Y.S., Song, Y., Sarmah, A., Li, X., Tack, F.M., 2018. Sustainable in situ
484 remediation of recalcitrant organic pollutants in groundwater with controlled release materials: A review.
485 *J. Control. Release.* 283, 200-213.

486 Pourakbar, M., Moussavi, G., Shekoohiyan, S., 2016. Homogenous VUV advanced oxidation process for
487 enhanced degradation and mineralization of antibiotics in contaminated water. *Ecotox. Environ. Safe.*
488 125, 72-77.

489 Rodríguez-Chueca, J., Laski, E., García-Cañibano, C., de Vidales, M.M., Encinas, Á., Kuch, B., Marugán, J.,
490 2018. Micropollutants removal by full-scale UV-C/sulfate radical based Advanced Oxidation Processes.
491 *Sci. Total Environ.* 630, 1216-1225.

492 Shi, X., Leong, K.Y., Ng, H.Y., 2017. Anaerobic treatment of pharmaceutical wastewater: a critical review.
493 *Bioresource Technol.* 245, 1238-1244.

494 Song, Y.N., Hou, D.Y., Zhang, J.L., O'Connor, D., Li, G.H., Cu, Q.B., Li, S.P., Liu, P., 2018. Environmental
495 and socio-economic sustainability appraisal of contaminated land remediation strategies: A case study at
496 a mega-site in China. *Sci. Total Environ.* 610, 391-401.

497 Sun, J.T., Zeng, Q., Tsang, D.C.W., Zhu, L.Z., Li, X.D., 2017. Antibiotics in the agricultural soils from the
498 Yangtze River Delta, China. *Chemosphere* 189, 301-308.

499 Tian, X., Jin, H., Nie, Y., Zhou, Z., Yang, C., Li, Y., Wang, Y., 2017. Heterogeneous Fenton-like degradation
500 of ofloxacin over a wide pH range of 3.6-10.0 over modified mesoporous iron oxide. *Chem. Eng. J.* 328,
501 397-405.

502 Xie, P., Yue, S., Ding, J., Wan, Y., Li, X., Ma, J., Wang, Z., 2018. Degradation of organic pollutants by
503 Vacuum-Ultraviolet (VUV): Kinetic model and efficiency. *Water Res.* 133, 69-78.

504 Urbano, V.R., Peres, M.S., Maniero, M.G., Guimarães, J.R., 2017. Abatement and toxicity reduction of
505 antimicrobials by UV/H₂O₂ process. *J. Environ. Manage.* 193, 439-447.

506 Wang, H., Zhang, L., Hu, C., Wang, X., Lyu, L., Sheng, G., 2018. Enhanced degradation of organic pollutants
507 over Cu-doped LaAlO₃ perovskite through heterogeneous Fenton-like reactions. *Chem. Eng. J.* 332,
508 572-581.

509 Wang, G., Wang, D., Dong, X., Zhang, X., Ma, H., 2017. Sodium persulfate based PVDF membrane for
510 concurrent advanced oxidation and ultrafiltration of ofloxacin in water. *Chem. Eng. J.* 315, 509-515.

511 Wu, Z., Guo, K., Fang, J., Yang, X., Xiao, H., Hou, S.D, Kong, X.J., Shang, C., Yang, X., Meng, F.A., Chen,
512 L.W., 2017. Factors affecting the roles of reactive species in the degradation of micropollutants by the
513 UV/chlorine process. *Water Res.* 126, 351-360.

514 Yan, B. and Niu, C.H., 2018. Adsorption behavior of norfloxacin and site energy distribution based on the
515 Dubinin-Astakhov isotherm. *Sci. Total Environ.* 631-632, 1525-1533.

516 Yang, Y., Pignatello, J.J., Ma, J., Mitch, W.A., 2014. Comparison of halide impacts on the efficiency of
517 contaminant degradation by sulfate and hydroxyl radical-based advanced oxidation processes (AOPs),
518 *Environ. Sci. Technol.* 48, 2344-2351.

519 Yin, K., Deng, L., Luo, J., Crittenden, J., Liu, C., Wei, Y., Wang, L., 2018. Destruction of phenicol antibiotics

520 using the UV/H₂O₂ process: Kinetics, byproducts, toxicity evaluation and trichloromethane formation
521 potential. Chem. Eng. J. 351, 867-877.

522 Yuval, A., Eran, F., Janin, W., Oliver, O., Yael, D., 2017. Photodegradation of micropollutants using V-
523 UV/UV-C processes; Triclosan as a model compound. Sci. Total Environ. 601, 397-404.

524 Yu, X.Y., Bao, Z.C., Barker, J.R., 2004. Free radical reactions involving Cl[•], Cl₂^{•-}, and SO₄^{•-} in the 248 nm
525 photolysis of aqueous solutions containing S₂O₈²⁻ and Cl. J. Phys. Chem. A 108, 295-308.

526 Zhang, P., Hou, D.Y., O'Connor, D., Li, X., Pehkonen, S.O., Varma, R.S., Wang, X., 2018. Green and size-
527 specific synthesis of stable Fe-Cu oxides as earth abundant adsorbents for malachite green removal. ACS
528 Sustain. Chem. Eng. 6, 9229-9236.

529 Zhu, X., Tsang, D.C.W., Chen, F., Li, S., Yang, X., 2015. Ciprofloxacin adsorption on graphene and granular
530 activated carbon: kinetics, isotherms, and effects of solution chemistry. Environ. Technol. 36, 3094-3102.